17th World Conference on Earthquake Engineering, 17WCEE
Sendai, Japan - September 13th to 18th 2020

SIMULATION ANALYSES OF STRONG GROUND MOTION OBSEREVED AT KiK-net MASHIKI STATION DURING THE 2016 KUMAMOTO EARTHQUAKE

K. Fukutake[(1)] , K. Yoshida[(2)], H. Kawase[(3)], F. Nagashima[(4)]

[(1)] *Principal Researcher, Ohsaki Research Institute, Inc., kiyoshi.fukutake@ohsaki.co.jp*
[(2)] *Principal Researcher, Ohsaki Research Institute, Inc., yoshida1@ohsaki.co.jp*
[(3)] *Professor, DPRI, Kyoto University, kawase.hiroshi.6x@kyoto-u.ac.jp*
[(4)] *Assistant Professor, DPRI, Kyoto University, nagashima.fumiaki.6v@kyoto-u.ac.jp*

Abstract

During the main shock of The 2016 Kumamoto Earthquake (*Mj* = 7.3), strong ground motion records exceeding 1000 cm/sec^2 were obtained at the vertical array of KiK-net Mashiki (KMMH16) observation point. In order to account for the strong ground motions, Nakagawa et al. conducted laboratory tests (dynamic deformation characteristics) of the actual ground at the Mashiki site, and performed simulation analyses of the observed records by using the one-dimensional equivalent linear wave propagation method.

The authors approximate the dynamic deformation characteristics obtained by Nakagawa et al. using two kinds of constitutive equations, the modified R-O (Ramberg-Osgood) model and the modified GHE (General Hyperbolic Equation) model, and are also carried out simulation analyses by using the one-dimensional nonlinear time history analysis method. As a result, although the calculated acceleration is slightly overestimated in the modified R-O model, the modified GHE model gives almost consistent results with the observation records. This indicates that fitting the constitutive equation to the dynamic deformation characteristics of the actual ground ($G/G_0 \sim \gamma$, $h \sim \gamma$ relationship) is important to reproduce the strong nonlinear ground response.

In addition, the authors have tried to introduce the scattering attenuation to improve the simulation accuracy especially in coda waves. Consequently, it is recognized that the consistency with the observed records becomes better when the scattering attenuation is considered in addition to the hysteresis attenuation due to the nonlinear loop.

Keywords: Kumamoto Earthquake; Array Records; Time History Nonlinear Analysis; Simulation; Scattering Attenuation

1. Introduction

During the main shock of The 2016 Kumamoto Earthquake (Mj = 7.3), strong ground motion records exceeding 1000 cm/sec^2 were obtained at the vertical array of KiK-net Mashiki (KMMH16) [1] observation point. In order to account for the strong ground motions, Nakagawa et al. [2] conducted laboratory tests (dynamic deformation characteristics) of the actual ground soil at the Mashiki site, and performed simulation analyses of the observed records by using the one-dimensional equivalent linear wave propagation method. In this paper, the authors try to approximate the dynamic deformation characteristics obtained by Nakagawa et al. [2] using two kinds of constitutive equations, the modified R-O (Ramberg-Osgood) model [3] and the modified GHE (General Hyperbolic Equation) model [4, 5], and are carried out simulation analyses by using one-dimensional nonlinear time history analysis method. The effects of the presence of scattering attenuation of the ground on the response are also examined.

2. Soil conditions

Table 1 shows soil conditions of KiK-net Mashiki site (KMMH16). Shear wave velocities (Vs) were determined by PS logging test presented in the reference [2]. It is found that relatively soft layers (No. 1 to 4) are existing above the hard layer (No. 5, Rock) of Vs 500m/s. The first and second natural periods of the soil layers are 0.91 and 0.41 seconds, respectively. The unit volume weight γ_t was estimated by the following equation [3].

$$\gamma_t = 9.8(1.4+0.67\sqrt{V_s}) \qquad V_s : \text{km/s} \tag{1}$$

Table 1 – Ground condition of KiK-net Mashiki (KMMH16)

No	GL m	Layer thickness m	Soil profile		γ_t kN/m^3	V_s m/s
1	3.0	3.0	non-linear, K-1	volcanic clay	15.9	110
2	9.0	6.0	non-linear, K-2	volcanic clay	16.9	240
3	14.0	5.0	non-linear, K-3	sand	16.9	240
4	15.0	1.0	non-linear, K-3	sand	16.9	240
5	33.0	18.0	linear	pumice tuff	18.4	500
6	41.0	8.0	non-linear	volcanic clay	17.9	400
7	51.0	10.0	non-linear	sand	19.4	760
8	69.0	18.0	non-linear	sandy gravel	19.4	760
9	101.0	32.0	linear	tuff breccia	19.7	820
10	133.0	32.0	linear	andesite rock	21.7	1470
11	143.0	10.0	linear	tuff breccia	19.2	700
12	167.0	24.0	linear	andesite rock	21.4	1380
13	200.4	33.4	linear	tuff	19.7	840
14	234.0	33.6	linear	andesite rock	21.7	1470
15	252.0	18.0	linear	andesite rock	24.5	2700

Nonlinear soil properties of layers Nos. 1 to 4 were examined by Nakagawa et al. [2] through the dynamic deformation tests. Nonlinear soil properties of layers Nos. 5 to 8 were not actually examined, and were approximately applied to those of layers Nos. 1 to 5. The other rock layers were assumed to be in the linear region. The bottom of the analysis model was fixed, and the underground observation wave was input at GL-252m as an E + F wave.

Figure 1 shows the results of dynamic deformation tests (plots) conducted by Nakagawa et al. [2] and fitting results using two types of constitutive equations (lines). The experimental values are characterized by a small damping factor *h* compared to that of standard cohesive soil or sandy soil, and particularly small in sandy soil. This is also pointed out by Nakagawa et al. [2]. The constitutive equations used are (1) modified R-O model [4] and (2) modified GHE model [5, 6]. Both are hysteresis function type models using the Masing rule, the modified R-O model is an exponential function type constitutive equation (including 3 parameters), and the modified GHE model is a hyperbolic type constitutive equation (including 10 parameters). The modified GHE model is in better agreement with the experimental results over a wide range of strain levels.

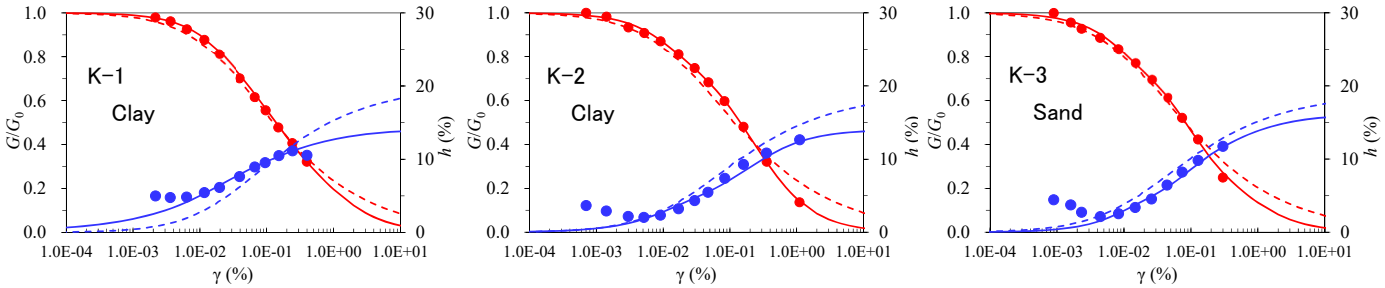

Fig. 1 – G/G_0~γ, h~γ relations of KiK-net Mashiki(KMMH16) and fitting of models
(●, ● : Experimental results, Broken lines : R-O model, Solid lines : GHE model)

3. Results and discussions of one-dimensional nonlinear analyses due to differences in constitutive equations

Figure 2 indicates a comparison of acceleration time histories of the EW components on the ground surface. It is recognized from this figure that the modified R-O model overestimates the acceleration amplitude. This is probably because the shear stiffness *G* becomes large in the large strain region of the $G/G_0 \sim \gamma$ relationship. In the modified GHE model, the peak at 5.6 seconds is underestimated, however, the amplitude is smaller than that of the modified R-O model, and corresponds well with the observation records. Because the modified GHE model is a hyperbola, it has a fracture asymptote. As stress approaches the asymptote, strain becomes large, resulting in greater hysteresis damping and lower acceleration amplitude (see below). Even in the modified GHE model, however, the analysis results are larger in 9 to 12 seconds. The cause of these phenomena may be considered the influence of scattering attenuation, which will be described later.

The maximum shear strain distribution along the vertical direction is depicted in Fig. 3. The sand layer (layer No. 3, 4) of *Vs*240m/s shows a large value. In particular, the maximum value is shown at the lower end of the layer of *Vs*240m/s. The difference between two models is remarkable in the layers Nos. 1 to 4. Compared with the modified R-O model, the modified GHE model gives larger strain in the layers No. 3 and 4, smaller strain in the layers No. 1 and 2. This may be considered a kind of seismic isolation effects due to the strong nonlinearity of the layers No. 3 and 4.

The shear stress/shear strain relationship of the sand layer No. 4 is shown in Fig.4. The maximum shear strain is about 2% in the modified R-O model, but it reaches 8% in the modified GHE model. Since the modified GHE model is a hyperbolic model and has a fracture line, the shear stress easily reaches to the peak

value, and the shear strain increases for that reason. As a result, it seems to be consistent with the acceleration records in Fig. 2.

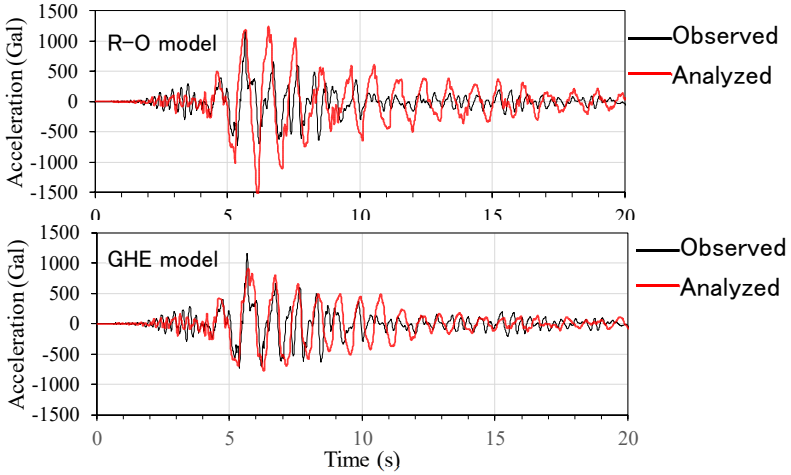

Fig. 2 – Comparison of observed records and analysis results of acceleration waveforms on the ground surface (EW component)

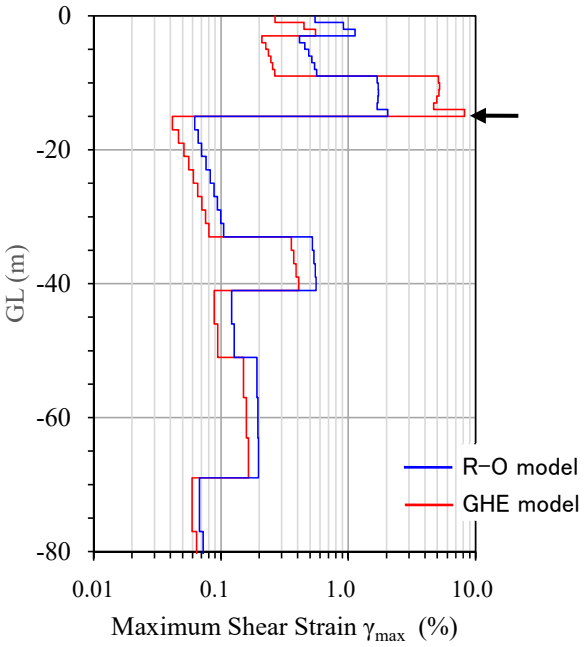

Fig. 3 – Distribution of maximum shear strain

4. Scattering attenuation

Ground attenuation includes hysteresis attenuation and scattering attenuation. In ordinary nonlinear analysis, only hysteresis attenuation is often considered. In this paper, it is assumed that the hysteresis attenuation is expressed by the nonlinear characteristics of the constitutive equation, and that the scattering attenuation is represented by the Rayleigh damping. The frequency-dependent scattering attenuation is used as follows by

Nakagawa et al.[6] In this case, the correction of the shear wave velocity using the equation (8) by Fukushima and Midorikawa [7] is not performed.

$$h = h_0 f^{\alpha} \qquad f\text{: frequency (Hz)} \tag{2}$$

h_0=0.07924, α=-0.46 for nonlinear layers

h_0=0.01377, α=-0.68 for linear layers

It should be noted that constant values are used for bands below 0.5 Hz and above 5 Hz. For the Rayleigh damping setting, the frequency range is set between 0.5 and 5.0 Hz, and it is assumed to coincide with the frequency-dependent damping at 5 Hz. Within that frequency range, coefficients are determined to minimize the sum of squares of absolute differences using frequencies as weighting values. In the equation $[C] = \alpha [M] + \beta [K]$, the following coefficients are obtained.

α=1.0315, β=0.001361 for nonlinear layers

α=0.1748, β=0.0001164 for linear layers

Figure 5 indicates a comparison between the frequency-dependent damping and the Rayleigh damping.

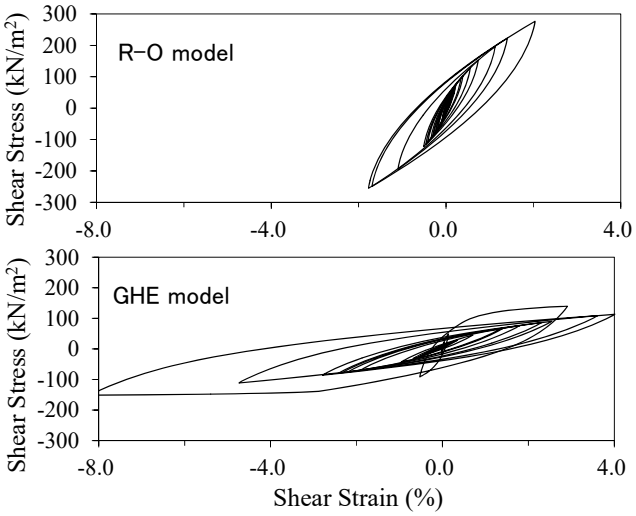

Fig. 4 – Shear stress-shear strain relationship
（GL-14m～-15m, Sand layer No.4、← in Fig. 3）

5. Results and discussions of one-dimensional nonlinear analyses considering scattering attenuation

Figure 6 shows a comparison of acceleration time histories of the EW component on the ground surface. Although the acceleration amplitude is overestimated without the scattering attenuation in the modified R-O model, the observation records are almost reproduced considering the scattering attenuation. The peak at the 6.2 seconds, however, is slightly overestimated. In particular, it can be seen that the scattering attenuation is effective in the subsequent acceleration time histories after 10 seconds when the strain level decreases and the hysteresis attenuation also becomes small. In the modified GHE model, the analysis results indicate larger values from 9 to 12 seconds without the scattering attenuation, however, considering the scattering attenuation, the agreement with the observed records shows fairly good except for the peak at 5.6 seconds. It is also

recognized that the response to the coda waves after 10 seconds is further improved in this case when taking account of the scattering attenuation. From the above, it is found that in the nonlinear analysis of the ground, it should be better to consider the scattering attenuation of the ground, which was rarely considered before, in addition to the hysteresis attenuation.

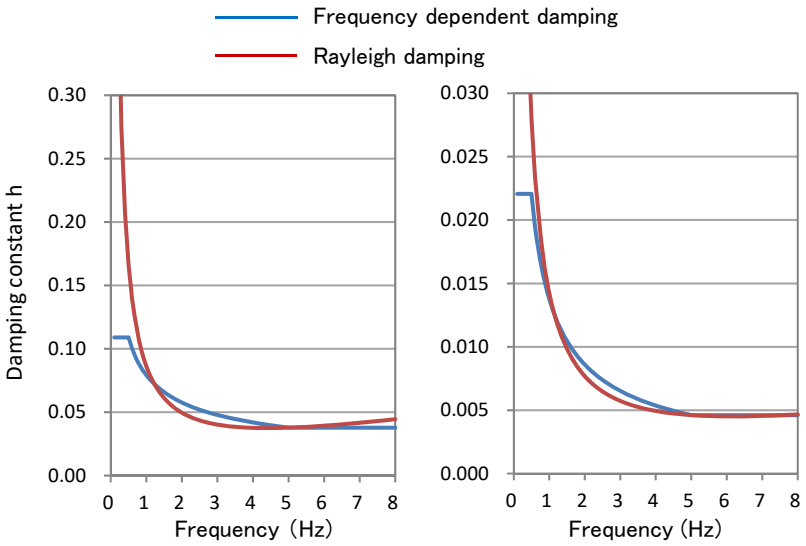

(a) Non-linear Layer (b) Linear Layer

Fig. 5 – Comparison of frequency dependent damping and Rayleigh damping

Figure 7 depicts a comparison of the acceleration response spectra (5% attenuation) of the EW component on the ground surface. At around 0.9 seconds, which corresponds to the major natural period of the ground, the analysis values are larger than the observed results, but it is clear that both of the constitutive models correspond better to the observed results when considering the scattering attenuation. It can be also recognized that the improvement is excellent in the long period region of 1 second or longer.

The maximum acceleration distribution in the vertical direction of the ground obtained by the analyses is illustrated in Fig. 8. The observed value on the ground surface is also shown in the figure for reference. In the modified R-O model, when the scattering attenuation is taken into consideration, the correspondence with the observed value on the ground surface becomes fairly good. When the waveform in Fig. 6 is examined in detail, however, it can be seen that the maximum value corresponds with the opposite phase. In the modified GHE model, large strain occurs in GL-14m to -15m (sand layer No. 4), and so-called seismic isolation effects are recognized. As a result, the response on the ground surface may be underestimated.

6. Conclusions

For the acceleration records observed at KiK-net Mashiki (KMMH16) during the main shock of The 2016 Kumamoto Earthquake, simulation analyses were carried out in this paper by using the nonlinear time history analysis method. In the analyses, two types of the constitutive equations were employed based on the dynamic deformation characteristics of the actual ground soil at Mashiki. To improve the simulation accuracy, the scattering attenuation was introduced in addition to the hysteresis attenuation due to the nonlinear loop. As a result, the following conclusions were obtained.

(1) Although the acceleration was slightly overestimated in the modified R-O model, the modified GHE model obtained results that were almost consistent with the observation records. This indicates that

fitting the constitutive equation to the dynamic deformation characteristics of the ground ($G/G_0 \sim \gamma$, $h \sim \gamma$ relationship) is important to reproduce the strong nonlinear response.

(2) Taking account of the scattering attenuation in addition to the hysteresis attenuation due to the nonlinear loop in the analyses gave better corresponding results to the observation records, especially in the coda waves.

In the future, we would like to execute effective stress analyses (liquefaction analyses using a bowl model) that can account for excess pore water pressure.

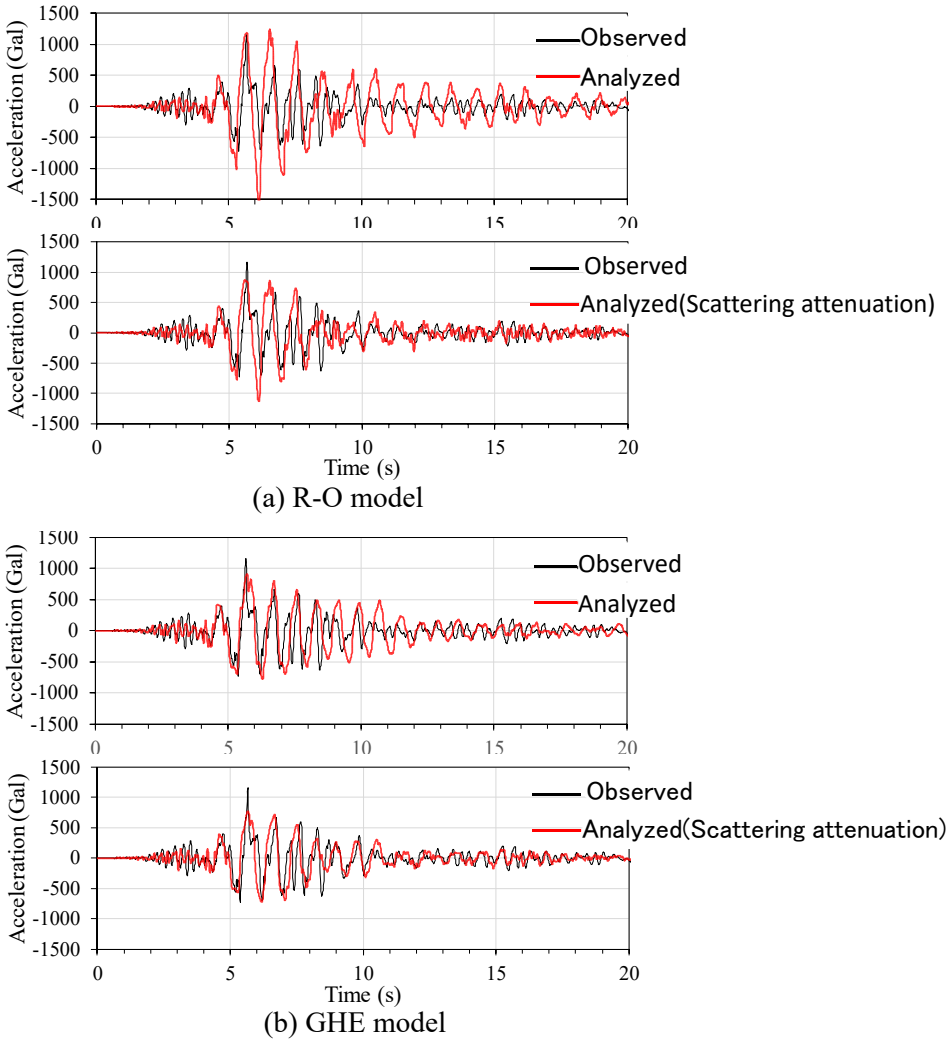

Fig. 6 – Comparison of observed records and analysis results of acceleration waveforms on the ground surface (EW component)

7. Acknowledgements

In this study, we have used earthquake observation records obtained and published by National Research Institute for Earth Science and Disaster Resilience (NIED), Japan. We would like to express our deep appreciation for NIED.

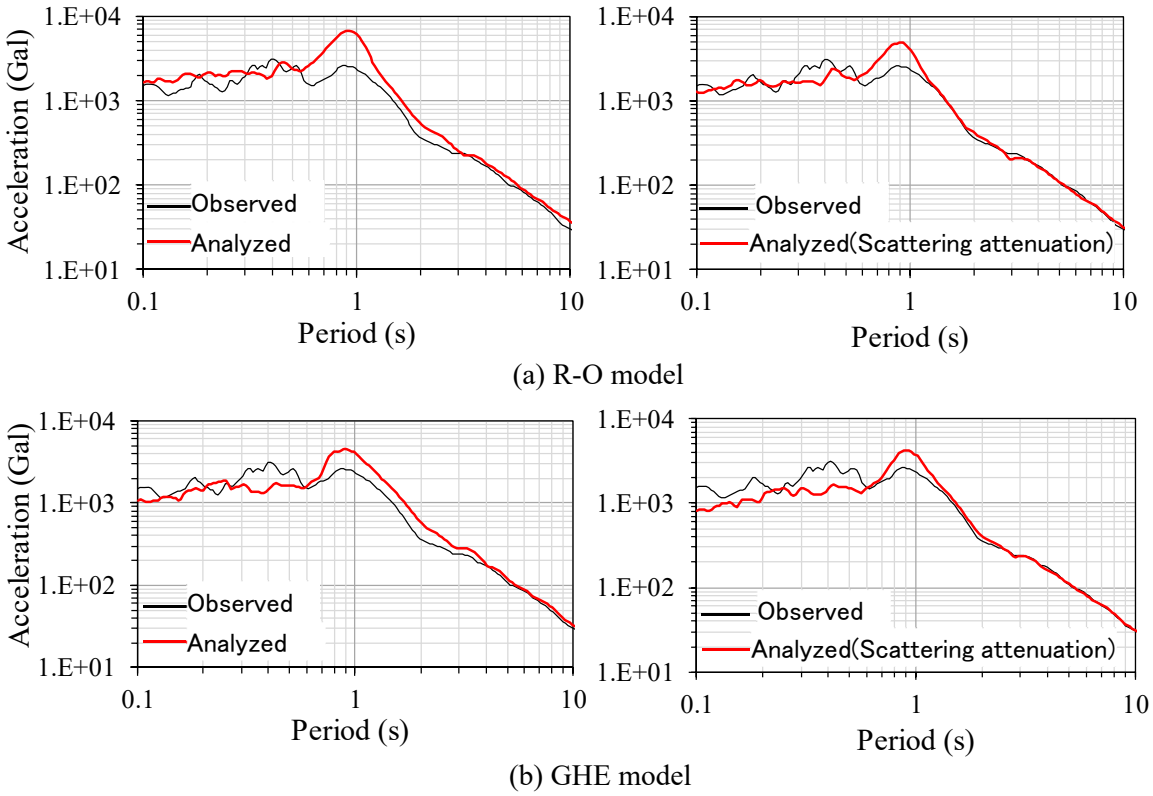

(a) R-O model

(b) GHE model

Fig. 7 – Response spectra on the ground surface（Damping 5%）

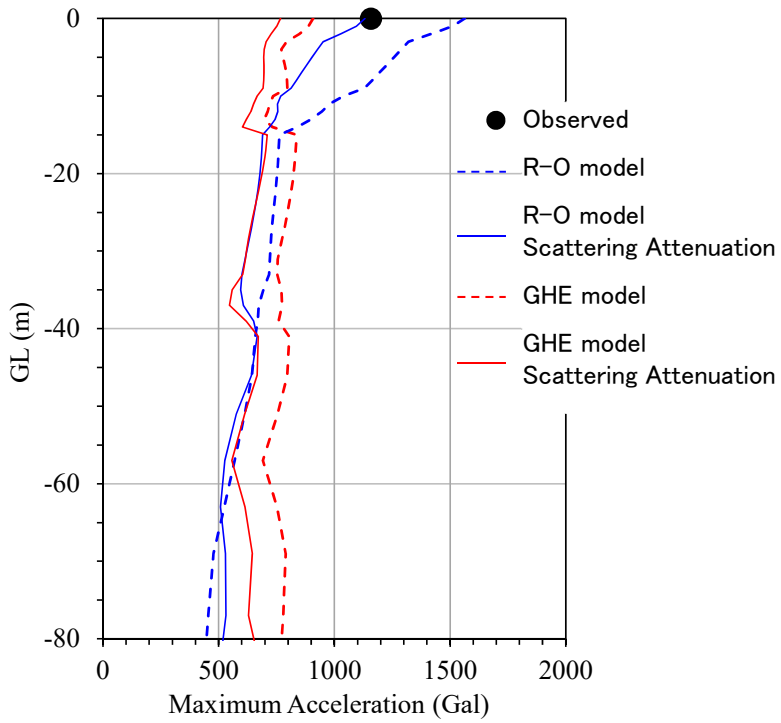

Fig. 8 – Distribution of maximum acceleration（EW component）

8. References

[1] National Research Institute for Earth Science and Disaster Resilience (K-NET, KiK-net) http://www.kyoshin.bosai.go.jp/kyoshin/

[2] Nakagawa H, Kashiwa N, Arai H (2017): Dynamic deformation characteristics and ground motion amplification characteristics of surface ground at the center region of Mashiki town, proc. of JAEE annual meeting, 1-8

[3] Kobayashi K, Abe Y, Uetake T, Mashimo M, Kobayashi H (1995): Inversion of Spectrum Ratio of Horizontal to Vertical Component of Preliminary Tremors. Proceedings of Architectural Institute of Japan, B-1, 307-308.

[4] Tatsuoka F, Fukushima S (1978): Stress-Strain Relation of Sand for Irregular Cyclic Excitation (1), Institute of Industrial Science. University of Tokyo, Vol.30, No.9, 26-29.

[5] Tatsuoka F, Shibuya S (1992): Deformation characteristics of soils and rocks from field and laboratory tests, Theme Lecture1, Proc. of the Ninth Asian Regional Conference on Soil Mechanics and Foundation Engineering, Vol. 2, 101-170

[6] Murono Y (1999): A Study on the Seismic Design Method of Pile Foundations That Reflects the Non-linear Dynamic Interaction During Strong Ground motions, Chapter 3, Report of Railway Technical Research Institute.

[7] Fukushima M, Midorikawa S (1994): Evaluation of Site Amplification Factors Based on Average Characteristics of Frequency Dependent Q-1 of Sedimentary Strata, The Architectural Institute of Japan's Journal of Structural and Construction Engineering, Vol.460, 37-46

